



LUND UNIVERSITY

Performance Analysis and Comparison between Aluminum and Graphite Foam Heat Exchangers under Countercurrent Flow Conditions

Lin, Wamei; Yuan, Jinliang; Sundén, Bengt

2011

[Link to publication](#)

Citation for published version (APA):

Lin, W., Yuan, J., & Sundén, B. (2011). *Performance Analysis and Comparison between Aluminum and Graphite Foam Heat Exchangers under Countercurrent Flow Conditions*. Paper presented at 2011 International Workshop on Heat Transfer Advances for Energy Conservation and Pollution Control, Xi'an, China.

Total number of authors:

3

General rights

Unless other specific re-use rights are stated the following general rights apply:

Copyright and moral rights for the publications made accessible in the public portal are retained by the authors and/or other copyright owners and it is a condition of accessing publications that users recognise and abide by the legal requirements associated with these rights.

- Users may download and print one copy of any publication from the public portal for the purpose of private study or research.
- You may not further distribute the material or use it for any profit-making activity or commercial gain
- You may freely distribute the URL identifying the publication in the public portal

Read more about Creative commons licenses: <https://creativecommons.org/licenses/>

Take down policy

If you believe that this document breaches copyright please contact us providing details, and we will remove access to the work immediately and investigate your claim.

LUND UNIVERSITY

PO Box 117
221 00 Lund
+46 46-222 00 00

Performance Analysis and Comparison between Aluminum and Graphite Foam Heat Exchangers under Countercurrent Flow Conditions

Wamei Lin, Jinliang Yuan, Bengt Sundén*

Department of Energy Sciences, Lund University, P. O. Box 118, Lund, 22100, Sweden

e-mail: bengt.sunden@energy.lth.se

ABSTRACT

Cross flow heat exchangers made in aluminum are common for radiators in vehicles. However, due to the increasing power requirement and the limited available space in the vehicles, it is extremely difficult to increase the size of the heat exchangers placed in the front of the vehicles. Placing the heat exchanger at the roof or the underbody of the vehicles might increase the possibility to increase the size of the heat exchangers. In this case, a new configuration of the heat exchangers has to be developed to accommodate the position change. In this paper, a countercurrent heat exchanger is proposed for the position on the roof of the vehicle compartment. Furthermore, a new material - graphite foam, which has high thermal conductivity (1700 W/(m.K)) and low density (0.2 to 0.6 g/cm^3), is a potential material for heat exchangers in vehicles. In order to evaluate the performance of the graphite foam heat exchanger, the CFD (computational fluid dynamics) approach is applied in a comparative study between the graphite foam and the aluminum heat exchangers under countercurrent flow. The comparison is conducted for the thermal performance (heat transfer coefficient) and the pressure loss. A performance factor COP (coefficient of performance) is presented and discussed too. Useful recommendations are highlighted and provided to promote the development of these kinds of heat exchangers in vehicles. [Keywords: countercurrent flow; heat exchanger; graphite foam]

INTRODUCTION

Due to the increasing power requirement and the limited available space in the vehicles, it is extremely difficult to increase the size of the radiators placed in the front of the vehicles. An idea suggested some time ago is to place the heat exchangers (HEXs) at the underbody of vehicles. Most public buses have the engine radiators at the underbody. That is due to the position of the engine (at the rear of the bus). However, the engine of other vehicles is placed in the front instead of at the rear. Recently, the Centro Ricerche Fiat [1] tried to use some

parts of the vehicle body panels as HEXs to reduce the radiator size in the light duty vehicles. Two roll bond HEXs installed on the engine hood and below the engine could dissipate 60 % of heat from the engine in all the test conditions. For the heavy duty vehicles, the radiator is always placed in the front of the vehicle, as shown in Fig. 1. A possible position for placing the radiator might be on the roof. If the radiator is placed at the roof (as shown in Fig. 1), the coolant flow direction and the air flow direction are opposite. This is a typical principle of a countercurrent flow HEX [2]. In the vehicle industry, the engine radiator is mostly a cross flow HEX. Based on the HEX design theory, a countercurrent flow HEX generally has better thermal performance than does a cross flow HEX. Thus, placing a countercurrent flow HEX on the roof of the truck driver compartment might be a good option for the engine radiator.

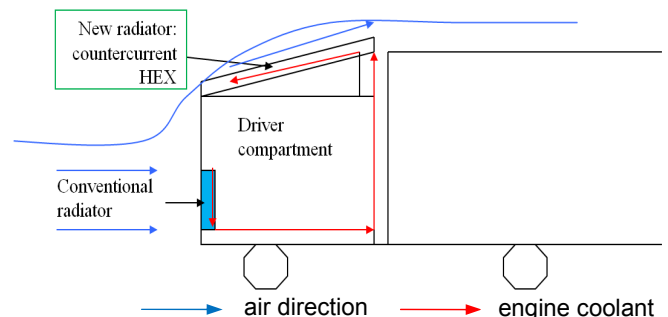


Figure 1 Schematics of the positions of a radiator in truck

Another method to increase the thermal performance of HEX is to use microcellular foam materials. A lot of research have been focused on the aluminum foam HEX [3-8]. However, the porous aluminum only presented a similar thermal performance with the conventional louvered fin. Meanwhile, the pressure drop was higher in the aluminum foam than in the louvered fin [4]. Another interesting foam material is graphite foam, whose effective thermal conductivity (40 to 150 W/(m.K)) [9] is much higher than that of the aluminum foam (2

NOMENCLATURE

A	area [m ²]
A_0	fin surface area [m ²]
C_F	Forchheimer coefficient
c_p	air specific heat [J.kg ⁻¹ .K ⁻¹]
f	friction factor
h	heat transfer coefficient [W.m ² .K ⁻¹]
k	turbulent kinetic energy
m	mass [kg]
P_k	turbulence production term
P_{pum}	pumping power [W]
Pr	Prandtl number
p	pressure [Pa]
Q	amount of heat energy [W]
S_i	source tem
St	Stanton number
T	temperature [K]
u	velocity [m.s ⁻¹]
V	volume [m ³]
ΔP	pressure drop [Pa]
ΔT	log mean temperature difference [K]

Greek Symbols

α	permeability [m ²]
γ	area to volume ratio [m ² .m ⁻³]
δ	turbulent index (turbulent $\delta=1$; laminar $\delta=0$)
ε	rate of energy dissipation
ϵ	porosity
μ	dynamic viscosity [Pa.s]
ρ	density [kg.m ⁻³]

Subscripts

<i>air</i>	air
<i>eff</i>	effective
<i>f</i>	fluid
<i>in</i>	inlet
<i>max</i>	maximum
<i>min</i>	minimum
<i>out</i>	outlet
<i>t</i>	turbulent
<i>water</i>	water

to 26 W/(m.K)) [5]. Besides that, the graphite foam has low density (0.2 to 0.6 g/cm³) and large specific surface area (5000 to 50000 m²/m³) [10-11].

The graphite foam is a potential material for heat exchangers, due to its high thermal performance. Klett et al. [12] designed a radiator with carbon foam. The cross section of the automotive radiator was reduced from 48 cm x 69 cm to 20 cm x 20 cm. The reduced size can decrease the overall weight, cost and volume of the system. Yu et al. [13] proved that the thermal performance of a carbon foam finned tube radiator could be improved by 15 %, compared to a conventional aluminum finned tube radiator, without changing the frontal area, or the air flow rate and pressure drop. Furthermore, Garrity et al. [14] found that the carbon foam samples brought away more heat than the multilouvered fin, when the volume of the heat exchangers was the same. However, there is high pressure drop through the graphite foam, due to the large hydrodynamic loss

associated with the open pores in the graphite foam [15]. An appropriate configuration of the foam can reduce the pressure drop [16]. For instance, Lin et al. [17] proved that a corrugated foam could reduce the pressure drop and maintain a high heat transfer coefficient. However, the coefficient of performance (COP, a ratio of the removed heat to the input pumping power) of the corrugated foam is lower than that of aluminum louver fin [18].

In order to develop a new HEX to resolve the cooling problems in the vehicle, a countercurrent flow HEX might be introduced and placed on the roof of a heavy duty vehicle. The HEX might be made of graphite foam. To reduce the pressure drop of graphite foam HEX, a triangular corrugated configuration will be applied to the foam on the air side of HEX. On the other hand, a comparison between the graphite foam and the aluminum heat exchangers under the countercurrent flow is carried out by CFD, to evaluate the thermal performance and the flow characteristics. Finally, the coefficient of performance (COP, a ratio of the removed heat to the input pumping power) is analyzed.

PHYSICAL MODEL

A simplified configuration of the countercurrent flow HEX is shown in Fig. 2. The water flows from the right to left side. However, the air flow direction (from left to right side) is opposite to the direction of water, as shown in Fig. 2 (a). The graphite foam and aluminum louver fin are placed between two water tubes as fin, respectively, as shown in Figs. 2 (b) and (c). The fluid is assumed to be incompressible with constant properties, and the flow is steady-state. The thermal resistance between the water tubes and the fins is neglected. In order to simplify the simulation model and save computational time, only a core of the HEX fin height is adopted, as shown in Fig. 2. The overall size of the core of graphite foam fin is: 49.7 mm x 6.85 mm x 70 mm (W*H*L). The size of aluminum louver fin is: 2.31 mm x 6.85 mm x 70.00 mm (W*H*L). The detailed configurations are shown in Table 1. Furthermore, the parameters of graphite foam are presented in Table 2.

Table 1. Sizes of aluminum louver fin and graphite foam fin.

Aluminum louver fin [19]	Fin pitch (mm)	Fin thickness (mm)	Louver spacing (mm)	Louver angle (θ)
	2.31	0.152	4.76	17.06
Graphite foam fin	Fin height (mm)	Fin thickness (mm)	Wave length (mm)	Double wave amplitude (mm)
	6.75	3	49.7	70

Table 2. Parameters of graphite foam [15].

Porosity	Effective thermal conductivity (W/(m.K))	Density (kg/m ³)	Area to volume ratio (m ² /m ³)	Permeability (m ²)	Forcheimer coefficient
0.82	120	500	5420	6.13×10^{-10}	0.4457

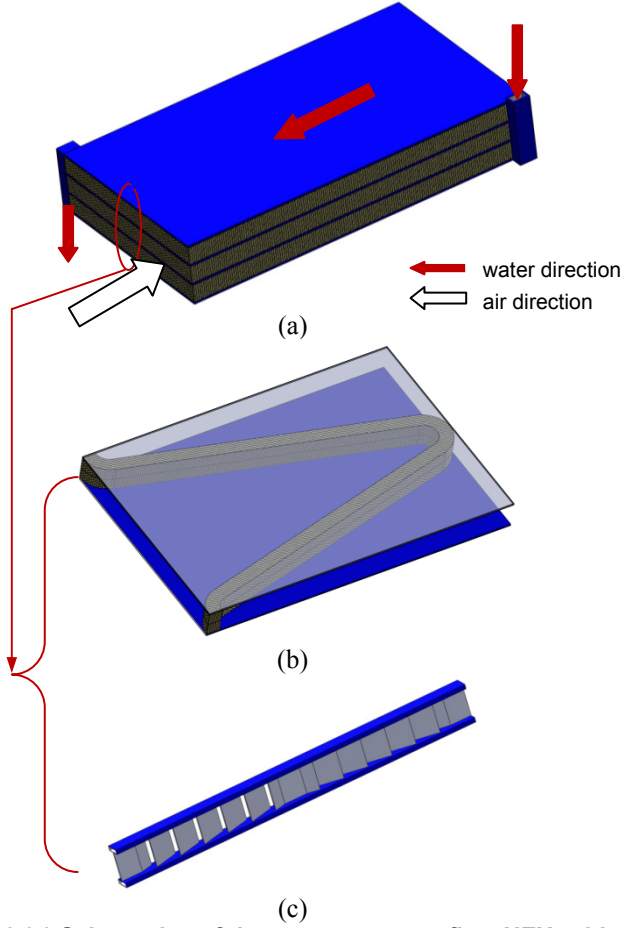


Figure 2 (a) Schematics of the countercurrent flow HEX, with (b) graphite foam fin, and (c) aluminum louver fin core.

MATHEMATICAL FORMULATION AND NUMERICAL METHOD

Adoption of flow model

Based on the velocity of heavy vehicles, the air inlet velocity of the countercurrent flow HEX in the simulation is ranging from 50 to 70 km/h. In this case, the Reynolds number on the air side is ranging from 2400 to 5000. Thus, low Reynolds number turbulent flow prevails on the air side. In order to capture the low Reynolds characteristics in the turbulent flow, the “renormalization group” (RNG) k - ϵ turbulence model is adopted [20-21] on the air side. However, laminar flow prevails inside the graphite foam. This is so because it is difficult to generate turbulent eddies in the small open cells of the graphite foam. Furthermore, laminar flow is considered on the water side as well, in order to simplify the simulation model (The inlet velocity of water is assumed to be less than 2 m/s.).

Mathematical formulation

Based on the above mentioned assumptions, the governing equations for continuity, momentum and energy can be expressed as follows [22-24]:

Continuity equation:

$$\frac{\partial(\rho_f \cdot u_i)}{\partial x_i} = 0 \quad (1)$$

Momentum equations:

$$\frac{\partial(\rho_f \cdot u_i u_j)}{\partial x_j} = -\epsilon \frac{\partial p}{\partial x_i} + \frac{\partial}{\partial x_j} \left((\mu_f + \delta \mu_t) \left(\frac{\partial u_i}{\partial x_j} + \frac{\partial u_j}{\partial x_i} \right) \right) + \epsilon S_i \quad (2)$$

Energy equation:

$$\frac{\partial(\rho_f \cdot u_i T)}{\partial x_i} = \frac{\partial}{\partial x_i} \left(\left(\frac{\mu_f}{Pr_f} + \delta \frac{\mu_t}{Pr_t} \right) \frac{\partial T}{\partial x_i} \right) \quad (3)$$

The heat transfer in porous media (graphite foam zone) is under the assumption of a local thermal equilibrium between fluid and solid phases. The different terms in the governing equations are defined differently in the air zone, water zone, and graphite foam zone, as shown in Table 3.

Table 3. Parameters definition in different zones.

parameter	Air zone	Water zone	Graphite foam zone
ρ_f	ρ_{air}	ρ_{water}	ρ_{air}
μ_f	μ_{air}	μ_{water}	μ_{air}
Pr_f	Pr_{air}	Pr_{water}	$\frac{\mu_{air} \cdot c_{p,eff}}{k_{eff}}$ where, $c_{p,eff} = \epsilon c_{p,air}$
S_i	0	0	$-\left(\frac{\mu_{air}}{\alpha} u_i + \frac{\rho_{air} C_F}{\sqrt{\alpha}} u u_i \right)$ (based on Forchheimer extended Darcy's equation)
δ	1	0	0
ϵ	1	1	0.82

For the air side, the equations of turbulent kinetic energy k and the rate of energy dissipation ϵ corresponding to the RNG k - ϵ turbulence model are:

Turbulent kinetic energy k equation:

$$\frac{\partial}{\partial x_i} (\rho k u_i) = \frac{\partial}{\partial x_j} \left(\left(\mu + \frac{\mu_t}{\sigma_k} \right) \frac{\partial k}{\partial x_j} \right) + P_k - \rho \epsilon \quad (4)$$

Rate of energy dissipation ϵ equation:

$$\frac{\partial}{\partial x_i} (\rho \epsilon u_i) = \frac{\partial}{\partial x_j} \left(\left(\mu + \frac{\mu_t}{\sigma_\epsilon} \right) \frac{\partial \epsilon}{\partial x_j} \right) + C_{1\epsilon} \frac{\epsilon}{k} P_k - C_{2\epsilon}^* \rho \frac{\epsilon^2}{k} \quad (5)$$

$$\text{where } C_{2\epsilon}^* = C_{2\epsilon} + \frac{C_{\mu} \eta^3 (1 - \eta/\eta_0)}{1 + \beta \eta^3}, \quad \mu_t = \rho C_{\mu} \frac{k^2}{\epsilon}$$

$$\text{and } \eta = Sk/\epsilon \text{ and } S = (2S_{ij}S_{ij})^{1/2}$$

The values of all of the constants are as follows:

$$C_{\mu} = 0.0845; \quad \sigma_k = 0.7194; \quad \sigma_\epsilon = 0.7194; \\ C_{\epsilon 1} = 1.42; \quad C_{\epsilon 2} = 1.68; \quad \eta_0 = 4.38; \quad \beta = 0.012$$

Computational domain and boundary conditions

Only half of the fin height is simulated, due to the symmetry in the fin height direction. The water tube is also simulated half height. Moreover, in order to get a uniform entry velocity for the HEX, the computational domain is extended upstream two times the length of the HEX. The downstream region of the HEX is also extended two times the HEX length, to eliminate the effect of outlet on the flow inside of HEX. Thus the total length of the computational domain is five times the length of the HEX, as shown in Fig. 3.

Because there are air and water zones in this simulation, the boundary conditions should be specified in the different zones separately.

- (1) Air zone
 - a) Upstream region: top-, front- and back sides are symmetry surfaces; left side is the velocity inlet.
 - b) Downstream region: top-, front- and back sides are symmetry surfaces; right side is the outlet.
 - c) HEX region: top side is symmetry surface; front side and back side are periodic for louver fin (due to the geometry of louver fin being not symmetry). However, front and back side are symmetry surfaces for the graphite foam fin.
- (2) Water zone
 - a) Upstream region: bottom-, front- and back sides are symmetry surfaces; left side is the outlet.
 - b) Downstream region: bottom-, front- and back sides are symmetry surfaces; right side is the velocity inlet (the temperature difference between the air inlet and the water inlet is set to 50 °C).
 - c) HEX region: bottom-, front- and back sides are symmetry surfaces.

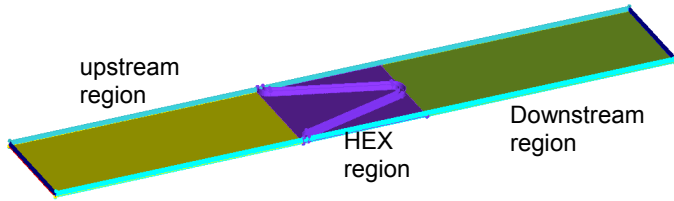


Figure 3 Computational domain of graphite foam fin.

Numerical method

The commercial code ANSYS FLUENT 12.0 is used for the numerical solution. A finite volume method (FVM) is adopted to convert the governing equations to algebraic equations so that they can be solved numerically [25]. The SIMPLE algorithm is used to couple pressure and velocity. A second-order upwind scheme is used for the space discretization of the momentum, energy and turbulence equations in the simulations. The convergence criterion for continuity, momentum, k and ε equations is below 10^{-3} . However, the convergence criterion for energy is below 10^{-8} , in order to ensure the energy balance between the air zone and the water zone under countercurrent flow.

The mesh generation is carried out by the ICEM. In order to achieve grid independence, three sets of mesh size (150-100-21; 139-100-21; 139-100-15) are built for the graphite foam HEX region in the air zone. Mesh sizes (150-100-5, 139-100-5, 139-100-3) are for HEX region in the water zone. The comparison of pressure drop and heat transfer coefficient among the three sets of mesh size shows that: the variation of pressure drop is between 1.5 % – 2.2 % in the graphite foam HEX region of the air zone, 0.013 % - 0.35 % in the HEX region of the water zone. The variation of heat transfer coefficient is between 0.25 % – 0.05 % in the graphite foam HEX region of the air zone, 0.064 % - 0.33 % in the HEX region of the water zone (when the air inlet velocity is 18 m/s and the water inlet speed is 1.5 m/s). Thus, the mesh size of 139-100-21 is adopted for the graphite foam fin in the air zone, and 139-100-5 is for the water

zone core. Moreover, the same method is adopted to check the grid independence of the aluminum louver fin simulation.

RESULTS AND DISCUSSION

Parameter definitions

Before presenting the simulation results, some parameters have to be defined. The first one is the heat transfer coefficient, which reads:

$$h = \frac{Q}{A_0 \Delta T} \quad (6)$$

where,

$$Q = m_f c_p (T_{out} - T_{in}) \quad (7)$$

$$\Delta T = \frac{\Delta T_{max} - \Delta T_{min}}{\ln \frac{\Delta T_{max}}{\Delta T_{min}}} \quad (8)$$

$$\Delta T_{max} = \max(T_{out.water} - T_{in.air}, T_{in.water} - T_{out.air}) \quad (9)$$

$$\Delta T_{min} = \min(T_{out.water} - T_{in.air}, T_{in.water} - T_{out.air}) \quad (10)$$

where, A_0 is the fin surface area (m^2). In the graphite foam, $A_0 = \gamma V$ (γ is the area to volume ratio, m^2/m^3 ; V the volume of graphite foam, m^3).

On the other hand, the coefficient of performance (COP) is the ratio between the removed amount of heat and the required pumping power.

$$COP = \frac{Q}{P_{pum}} = \frac{Q}{u_{in.air} A_{in} \Delta p} \quad (11)$$

where, Δp is the air pressure drop through the countercurrent flow HEX (Pa).

Model validation

Prior to real calculation, the validation of the model has to be carried out. There are two simulation models in this paper. One is the graphite foam fin model, another one for the aluminum louver fin. The validation of the graphite foam model was carried out and presented in [18]. It was shown that the simulated pressure drop and the thermal performance of the graphite foam agreed satisfactorily with the experimental data. On the other hand, the aluminum louver fin model was validated by comparing with experimental results in [19]. The deviation between the simulation and the experimental results is shown in Table 4. The $StPr^{2/3}$ predicted by the RNG $k-\varepsilon$ turbulence model deviated less than 5.4 % from the experimental result. Moreover, the deviation of the friction factor f between the simulation and the experimental results is less than 4.1 %. Thus, there is a good agreement in the data for the aluminum louver fin, in terms of thermal performance and pressure drop.

Table 4. Deviation between the simulation results and the experimental data (aluminum louver fin).

Re	$StPr^{2/3}$ [19]	Simulation $StPr^{2/3}$	f in [19]	Simulation f
2837	0.0092	0.0097 (5.4 %)	0.0435	0.044 (1.1 %)
3392	0.0087	0.0086 (1.2 %)	0.041	0.04 (2.4 %)
3769	0.0082	0.0081 (1.2 %)	0.0398	0.0382 (4.1 %)

Performance comparison between the graphite foam fin and the aluminum louver fin

The thermal performance and pressure loss are two important factors in the heat exchanger design. In order to compare the performance of the graphite foam fin and the aluminum louver fin, the heat transfer coefficient is considered in the thermal performance. The pressure drop is used to analyze the flow characteristics. Finally, a composite parameter, COP, is highlighted.

(1) Thermal performance

The heat transfer coefficients predicted for the graphite foam fin and the aluminum louver fin are shown in Fig. 4. The heat transfer coefficients increase with the frontal velocity. Furthermore, the heat transfer coefficient in the graphite foam fin is increased faster than the one in the aluminum louver fin. Fig. 4 also shows that the heat transfer coefficient of the graphite foam fin is much higher than that of the aluminum louver fin. So there is a high thermal performance in the graphite foam fin. This is mostly because of the special structure of the graphite foam, in which there are many opening pores connected together. The air changes its direction very frequently by the inducement of the foam structure. In this case, the air can be mixed sufficiently in the graphite foam to increase the heat transfer coefficient. Meanwhile, there is an extremely high thermal conductivity in the graphite foam. The heat transfer inside the solid foam is so fast that there is high temperature difference between the air and fin wall. All these factors contribute to the high thermal performance of the graphite foam fin.

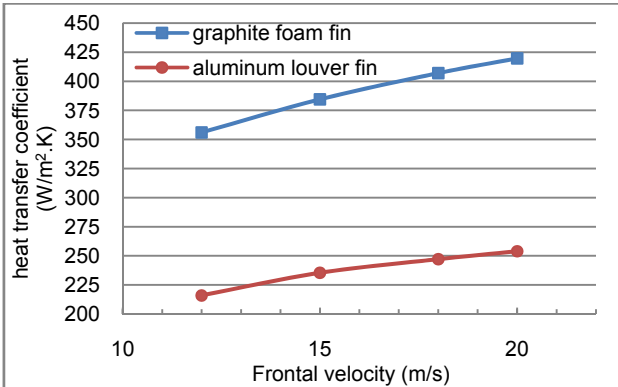


Figure 4 Heat transfer coefficients at different velocity.

(2) Pressure loss

The pressure loss through the graphite foam is based on Forchheimer extended Darcy's equation (the source term in Eq. (2)). Fig. 5 illuminates the pressure drop through the graphite foam fin and the aluminum louver fin as a function of frontal air velocity. The pressure drops increase with the frontal velocity. However, the pressure drop through the graphite foam is much higher than that through the aluminum louver fin. Meanwhile, the pressure drop is increasing extremely faster in the graphite foam than the one in the aluminum louver fin. It implies a high flow resistance in the graphite foam. The high flow resistance in the porous graphite foam is associated with small size pores in the graphite foam. Moreover, the large internal surface in the graphite foam also increases the hydrodynamic loss. It is a fact

that the high flow resistance in the graphite foam fin is the major problem, compared to the aluminum louver fin.

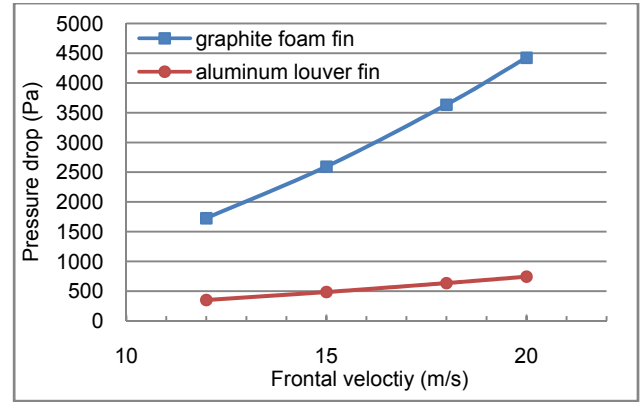


Figure 5 Pressure drops at different velocity.

(3) Coefficient of performance

There is a high heat transfer coefficient in the graphite foam fin (as shown in Fig. 4), together with a high pressure drop as in Fig. 5. In order to compare the graphite foam fin with the aluminum louver fin in an appropriate method, the coefficient of performance (COP) is adopted. The definition of COP is shown in Eq. (11). The simulation results of COP are shown in Fig. 6. There is high thermal performance in the graphite foam fin, but due to the extremely high flow resistance in the graphite foam, the COP of graphite foam is lower than that in the aluminum louver fin. On the other hand, the COP values are reduced when the velocity is increased. The COP of the aluminum louver fin is reduced faster than the one in the graphite foam fin. By increasing the velocity, the difference of COP between the graphite foam fin and the aluminum louver fin is reduced. However, it is difficult to reach the same COP as for the aluminum louver fin by the graphite foam fin by increasing the velocity, as shown in Fig. 6.

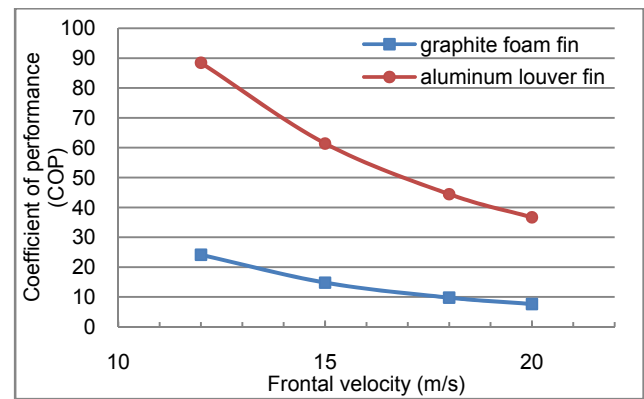


Figure 6 Coefficient of performance at different velocity.

A case analysis between a graphite foam HEX and an aluminum louver fin HEX under countercurrent flow

In order to evaluate the performance difference between a graphite foam HEX and an aluminum louver fin HEX under countercurrent flow, a case study (a truck with 200 kW cooling power) is carried out. The operating data about this case is shown in Table 5.

After analyzing this case, the total cooling surface required for the aluminum louver fin is 17.1 m^2 , and 11.75 m^2 for the graphite foam HEX (as shown in Table 6). The total volume of the graphite foam HEX is 0.0114 m^3 , which is 45.6 % less than the one of the aluminum louver fin HEX (0.021 m^3). Meanwhile, the weight of the graphite foam HEX is 1.12 kg, which is 65 % lower than that of the aluminum louver fin HEX (only considering the weight in the air side). However, due to the high flow resistance in the graphite foam, the power for forcing air through HEX is much higher in the graphite foam HEX than the one in the aluminum louver fin.

Table 5. Assumed operating data of a truck

Cooling power (kW)	200	
Truck speed (km/h)	65	
Radiator (water side)	$T_{in} = 90^\circ\text{C}$	$T_{out} = 85^\circ\text{C}$
Radiator (air side)	$T_{in} = 30^\circ\text{C}$	$T_{out} = 55^\circ\text{C}$

Table 6. Comparison between the graphite foam HEX and aluminum louver fin HEX under countercurrent flow

	Graphite foam HEX	Aluminum louver fin HEX
Cooling surface area (m^2)	11.75	17.1
Overall size ($\text{W}^*\text{H}^*\text{L}$) ($\text{mm}^*\text{mm}^*\text{mm}$)	1000*163*70	1000*300*70
Total volume (m^3)	0.0114	0.021
Weight of fins in air side (kg)	1.12	3.58
Power for forcing air through HEX (W)	7610	3434

CONCLUSION AND RECOMMENDATION

Because of the increased cooling requirement in vehicles, an advanced heat exchanger has to be developed in the vehicle industry. Placing the heat exchanger at a new place on vehicles, or using new material for heat exchanger might be in favor of the design of advanced heat exchangers. In this paper, a countercurrent flow HEX is presented for placement on the roof of the driver compartment. Furthermore, a performance comparison between graphite foam HEX and aluminum louver fin HEX under countercurrent flow is carried out. The major results are as follows:

- 1) Graphite foam fin design has higher heat transfer coefficient than does aluminum louver fin. Meanwhile the pressure drop through the graphite foam is much higher than that one through the aluminum louver fin.
- 2) Due to the large hydrodynamic losses in the graphite foam, the coefficient of performance (COP) in the graphite foam is lower than the one in the aluminum louver fin.
- 3) For the considered case in this paper, the volume of graphite foam HEX is 45.6 % less than the one of aluminum louver fin under the countercurrent flow. Meanwhile, the weight of graphite foam HEX is 65 % less than that one of aluminum louver fin.

However, there are still several problems facing the application of graphite foam HEX in vehicles.

- I. It requires large input pumping power for the graphite foam HEX. So an appropriate configuration of graphite foam has to be developed to reduce the pressure drop.

- II. The manufacturing methods of graphite foam HEX are not mature, compared to the one of aluminum HEX.

Thus, there is still much effort needed for the development of new heat exchangers in the vehicle industry.

ACKNOWLEDGMENT

The authors acknowledge the financial support from the Swedish Energy Agency and industries.

REFERENCES

- [1] Malvicino C., Mattiello F., Seccardini R. et al, Flat heat exchangers, Proceedings of the Vehicle Thermal Management Systems Conference & Exhibition 10, 2011: 91-98.
- [2] Shah R. K., Sekulic D. P., Fundamentals of Heat Exchanger Design. John Wiley & Sons, Inc. 2003.
- [3] Calmidi V. V., Mahajan R. L., The effective thermal conductivity of high porosity fibrous metal foams, Journal of Heat Transfer, 1999, 121: 466-471.
- [4] Kim S. Y., Paek J. W., Kang B. H., Flow and heat transfer correlations for porous fin in a plate-fin heat exchanger, Journal of Heat Transfer, 2000, 122: 572-578.
- [5] Paek J. W., Kang B. H., Kim S. Y., Hyum, J. M., Effective thermal conductivity and permeability of aluminum foam materials, International Journal of Thermophys, 2000, 21 (2): 453-464.
- [6] Boomsma K., Poulidakos D., On the effective thermal conductivity of a three-dimensionally structured fluid-saturated metal foam, International Journal of Heat and Mass Transfer, 2001, 44: 827-836.
- [7] Bhattacharya A., Calmidi V. V., Mahajan R. L., Thermophysical properties of high porosity metal foams, International Journal of Heat and Mass Transfer, 2002, 45: 1017-1031.
- [8] Mahjoob S., Vafai K., A synthesis of fluid and thermal transport models for metal foam heat exchangers, International Journal of Heat and Mass Transfer, 2008, 51: 3701-3711.
- [9] Klett J., Hardy R., Romine E., Walls C., Burchell T., High-thermal-conductivity mesophase-pitch-derived carbon foams: effect of precursor on structure and properties, Carbon, 2000, 38: 953-973.
- [10] Yu Q., Thompson B. E., Straatman A. G., A unit cube-based model for heat transfer and fluid flow in porous carbon foam, Journal of Heat Transfer, 2006, 128: 352-360.
- [11] Straatman A. G., Gallego N. G., Thompson B. E., Hangan H., Thermal characterization of porous carbon foam-convection in parallel flow, International Journal of Heat and Mass Transfer, 2006, 49: 1991-1998.
- [12] Klett J., Ott R., McMillan A., Heat exchangers for heavy vehicles utilizing high thermal conductivity graphite foams, SAE Paper 2000-01-2207, 2000.
- [13] Yu Q., Straatman A. G., Thompson B. E., Carbon-foam finned tubes in air-water heat exchangers, Applied Thermal Engineering, 2006, 26: 131-143.
- [14] Garrity P. T., Klausner J.F., Mei R., Performance of aluminum and carbon foams for air side heat transfer augmentation, Journal of Heat Transfer, 2010, 132: 121901
- [15] Straatman A. G., Gallego N. C., Yu Q., et al, Characterization of porous carbon foam as a material for compact recuperators, Journal of Engineering for Gas Turbines and Power, 2007, 129: 326-330.
- [16] Gallego N. G., Klett J. W., Carbon foams for thermal management, Carbon, 2003, 41: 1461-1466.
- [17] Lin Y. R., Du J. H., Wu W., Chow L. C., Notardonato W., Experimental study on heat transfer and pressure drop of recuperative heat exchangers using carbon foam, Journal of Heat Transfer, 2010, 132: 091902

- [18] Lin W. M., Sundén B., Graphite foam heat exchanger for vehicles, Proceedings of the Vehicle Thermal Management Systems Conference & Exhibition 10, 2011: 81-90.
- [19] Kays W. M., London A. L., Compact Heat Exchangers, 3rd edition, McGraw Hill Book, 1995.
- [20] Pope S. B., Turbulent Flows, Cambridge University, 2000.
- [21] ANSYS FLUENT 12.0 - Theory Guide, ANSYS, Inc., 2009.
- [22] Tannehill J. C., Anderson D. A., Pletcher R. H., Computational Fluid Mechanics and Heat Transfer, 2nd edition, Taylor & Francis, 1997.
- [23] Yuan J., Huang Y., Sundén B., Wang W., Analysis of parameter effects on chemical reaction couple transport phenomena in SOFC anodes, Heat Mass Transfer, 2009, 45: 471-484.
- [24] Lu W., Zhao C. Y., Tassou S. A., Thermal analysis on metal-foam filled heat exchangers. Part I: metal-foam filled pipes, International Journal of Heat and Mass Transfer, 2006, 49: 2751-2761.
- [25] Versteeg H. K., Malalasekera W., An Introduction to Computational Fluid Dynamics, 2nd edition, Pearson Prentice Hall, 2007.